JP Journal of Heat and Mass Transfer

http://www.pphmj.com
http://dx.doi.org/10.17654/HM014010047
Volume 14, Number 1, 2017, Pages 47-68 **ISSN: 0973-5763**

EXPERIMENTAL INVESTIGATION AND ANALYTICAL STUDY OF THE HEAT TRANSFER LIMITS OF A DOUBLE LAYER WRAPPED SCREEN MESH HEAT PIPE SYSTEM

Yogesh R. Mahulkar[1], C. M. Sedani[2] and Manoj K. Jadhav[3]

[1]IOKCOE SPPU Pune
India

[2]MSSCOET BAMU
Aurangabad, India

[3]SRCOE SPPU Pune
India

Abstract

Heat pipe has wide variety of application for thermal management, typically here use of heat pipe for 45 watt electronic part to maintain heat section temperature below 60°C to 70°C. The use of double layer mesh affords better result on single layer mesh heat pipes. For experimental results and analytical study, here diverse combination of double layer wrapped screen mesh is used with heat input to evaporator section of 45 watt. Darcy's law and Knudsen diffusion explain well the heat transfer and flow through porous media, through the help of this it observed to provide coarse mesh at outer side and fine pore mesh at inner side for the best performance of heat pipe. Discussion on Empirical analysis and CFD results with experimental results conclusion made the best combination of double layer wrapped

Received: April 23, 2016; Revised: June 11, 2016; Accepted: August 19, 2016
Keywords and phrases: heat pipe, double layer mesh, porosity, permeability, thermal resistance, heat transfer limits.

screen mesh for heat pipe afford to solve complex problems of heat and mass transfer.

1. Introduction

Biporous structure is used to improve the performance of heat pipe. The characteristics improvement shows with biporous evaporator, biporous wick, vaporization mechanism in biporous wicks, thermal performance analysis, biporous heat pipe module and monoporous wick. In biporous evaporator, the characteristics of capillary pressure and reducing dry out improve against the capillary limitation and boiling limitation. In biporous wick, the porous structure has two characteristics of pore sizes to improve the vaporization phenomenon. In vaporization mechanism in biporous wicks, the characteristics of evaporation vapor-liquid interface described with three regions of equilibrium thin film, transition and intrinsic regions. Furthermore, in the minor and big pores sizes, the liquid film formation increases with increase in the evaporation rate and reducing the formation of vapor blanket layer. Thermal performance analysis originates the low effective thermoconductivities of the biporous wick than the monoporous wick when heat flux at the evaporator is relatively low so used the pin fins surrounding to the surface for improved convective heat transfer. In biporous heat pipe module, the modules of the evaporator, vapor chamber and condenser described with the thermal resistances depend on the capillary force, boiling phenomenon and convection heat transfer [1]. Wick structure in heat pipe was prepared as biporous wick by applying copper nanoparticle film on copper microporous wick structure. Copper nanoparticle film is used being based on the fine pore radius to improve the capillary pressure, reduce permeability and increase vaporization rate. The experiments performed on the monoporous and biporous with nanolayer at inlet and outlet. The maximum capillary pressure observed with sample of biporous wick with nanolayer at outlet [2].

Focus on the measurement of properties of wick material of heat pipe for permeability and effective pore radius. The different tests are used for measurement of permeability and effective pore radius like risen and fallen meniscus tests for effective pore radius measurement, flow paths of liquid in

forced flow permeability tests, rate of rise wick property measurement test, data analysis using closed form solution, data analyzed of effect of error associated with temperature, porosity and evaporation and rate of mass uptake. Acetone rises the most rapidly than the heptanes and methanol and heptanes than methanol due to its low viscosity and higher surface tension [3]. The characterization of wicks of heat pipe with measurements of pore size, porosity and permeability of wicks improves performance of heat pipe. The pore size and porosity measured with mercury intrusion porosimeter which is used to calculate permeability that effect directly the flow resistance and heat transfer rate. The effect of sintering on porosity observed that porosity reduces with an increase in sintering time. The effect of sintering on pore size distribution obtained lower pore size with less sintering temperature. The effect of sintering on shrinkage of compacts shows at higher sintering temperature more shrinkage obtained due to filling gaps, removal spaces, form larger and uniform crystals which improve necking. Sintering wick heat pipe helps to optimize heat pipe performance as compared to the conventional heat pipe wicks [4].

The investigation of parameters of sintered heat pipe with lumped parameter model and found that wick dryness increases with decrease in the wick thickness. In addition, reducing the pipe diameter the heat pipe thermal resistance increases and the heating power working limit decreases. Grain radius has no effect on thermal resistance and thermal heat pipe performance but too small or too large grains promote a high degree of evaporation and influencing the working limits [5].

2. Experimental Setup

Figure 1. Heat pipe with cooling jacket at condenser side.

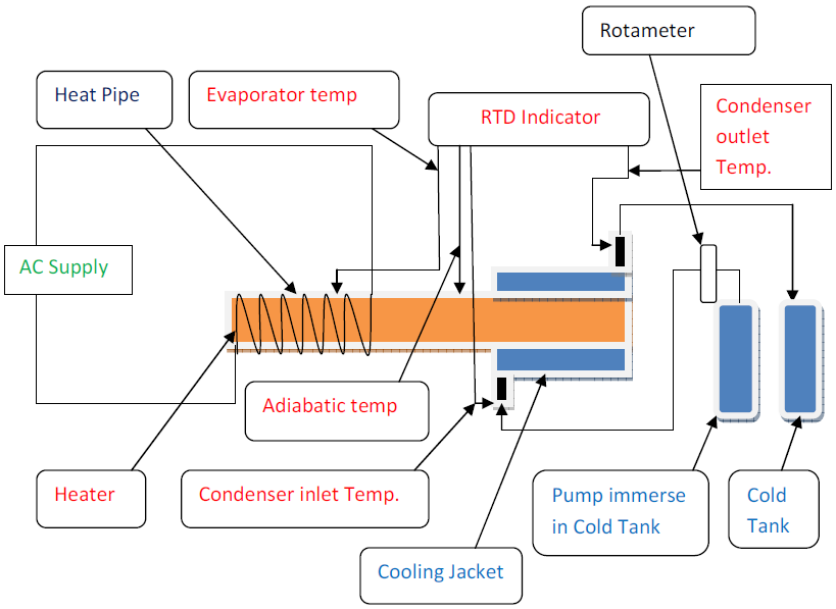

Figure 2. Experimental setup for testing double layer wrapped screen mesh heat pipe.

The experimental setup (Figure 2) shows the different components used for testing double layer wrapped screen mesh heat pipe using water as working fluid. Here 10 heat pipes are used for testing at different inclination with dissimilar double layer wrapped screen mesh heat pipe. Unlike 10 heat pipes with various combinations of outer mesh (wall side) and inner mesh (towards centre line of heat pipe or liquid side) of wrapped screen mesh wick. Dimmerstat control heat input to evaporator section with heating coils and rotameter control water flow through cooling jacket for cooling condenser section.

Table 1. Parameters same for all 10 heat pipes

Parameter	Specification	Parameter	Specification
Overall length of heat pipe	250mm	Mass flow rate of water	4ml/sec
Length of evaporator section	93.75mm	Heat input	45watt
Length of condenser section	93.75mm	Heat pipe material	Copper
Length of adiabatic section	62.5mm	Wick material	Phosphorus Bonze

Pipe diameter	12mm	Wick structure	Wrapped screen mesh
Pipe shape	Annular	At 90° inclination	evaporator section is exactly below the condenser section
Thickness of wick: 250 mesh	0.11mm	Thickness of wick: 180 mesh	0.12mm
Thickness of wick: 100 mesh	0.205mm	Thickness of wick: 60 mesh	0.35mm

3. Results and Discussion

The phase change driving mechanism during operation of heat pipe explicates with the help of operation mechanism, phase change driving model, heat transfer limitation and capillary wick heat pipe. In operation mechanism of a heat pipe with porous wick, the circulating working fluid should overcome the pressure drop of liquid flow and vapor flow and as well gravity. The driving mechanism of circulation of fluid is due to capillary force on evaporation and phase change driving force. The model of electrical analogy and mathematical model developed for the pressure head of liquid and vapor. In phase change driving model, the vapor phase has more energy than the liquid phase, besides the losses of energy and driving potential in vapor of heat pipe is more. To understand the vapor energy driving mechanism, the mathematical model used using energy equations and parameters. In heat transfer limitation, the working maximum heat flux depends upon the number of parameters and mathematical model elaborate the maximum heat flux. In capillary wick, the maximum capillary pressure, capillary pressure head, phase change driving pressure head, vapor flow resistance and liquid flow resistance values calculated and tabulated [6].

Flow and heat transfer characteristics of heat pipe analyzed using vapor phase analysis, liquid phase analysis, temperature distribution and operational criteria. Analytical results based on the Bernoulli’s equation, Reynolds number, Clausius-Clapeyron equation, Darcy’s law, operational

limit, thickness of the vapor space, different Reynolds number, different diameters, liquid pressure and vapor pressure of vapor velocity distribution analysis and pressure distribution analysis [7].

Properties of wick material deliberate for improvement in the performance of heat pipe. In wick material, forced flow permeability measurement, bubble point pore radius measurement, rate of rise property measurement using Darcy's equation with the discussion about effects of parameters are the pressure drop, capillary force, permeability, effective pore radius, fabrication process, pressure drop, flow rate, wick structure and heights of liquid. Experimental measurement of parameters done with forced flow experiment, bubble point test and rate of rise test [8].

Dryout of heat pipe with biporous wick investigate through different parameters like vapor flow induced droplet splash, vapor occupation of liquid transport passages, lost of liquid volume, heat fluxes, evaporator temperature and pressure drop [9].

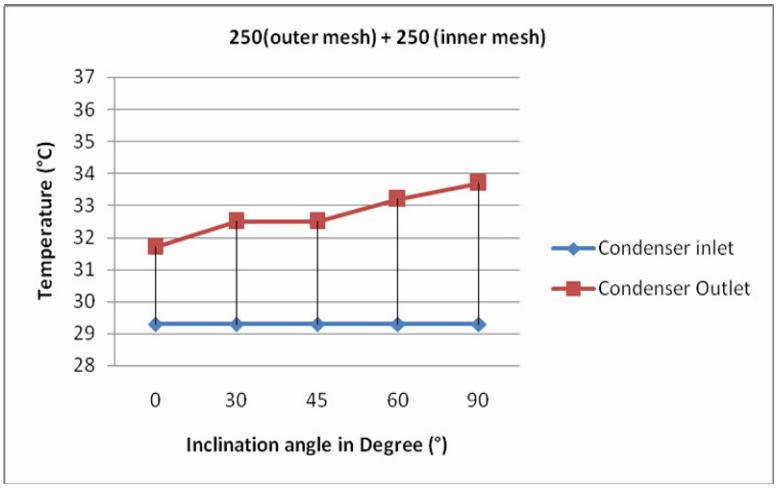

Figure 3. Double layer wrapped screen mesh wick with 250 (outer mesh) + 250 (inner mesh).

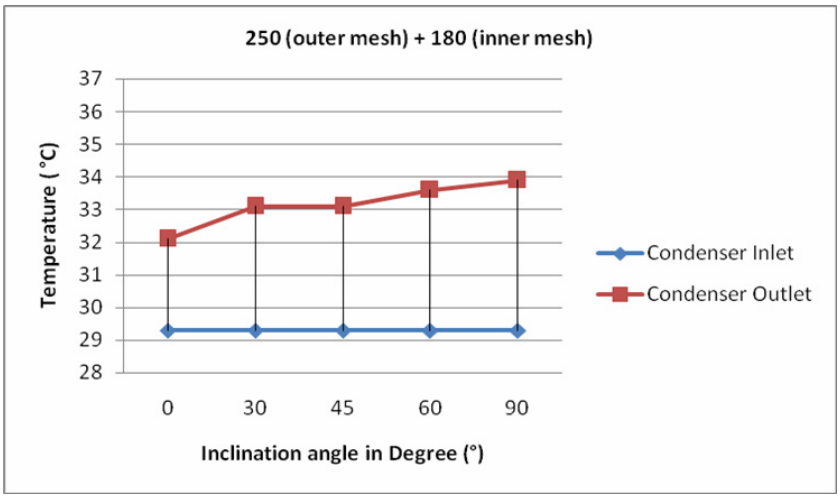

Figure 4. Double layer wrapped screen mesh wick with 250 (outer mesh) + 180 (inner mesh).

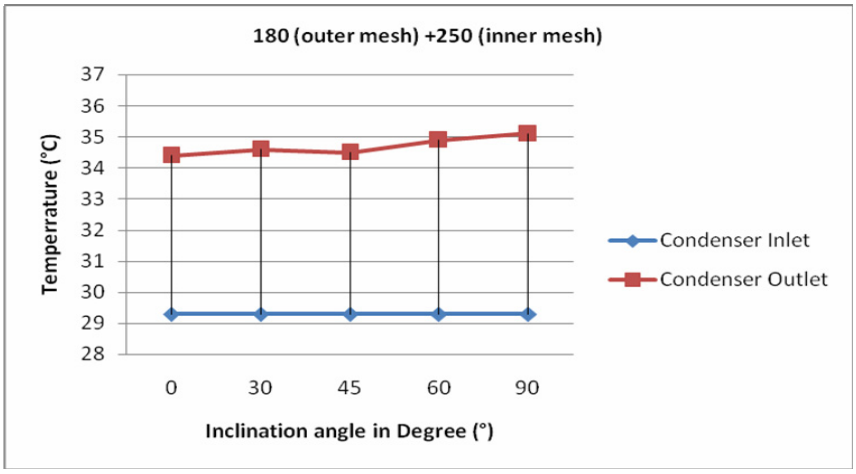

Figure 5. Double layer wrapped screen mesh wick with 180 (outer mesh) + 250 (inner mesh).

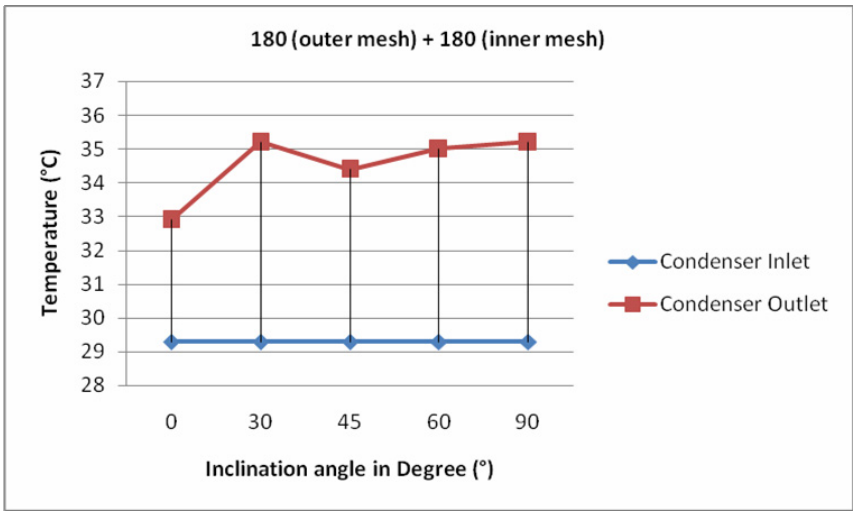

Figure 6. Double layer wrapped screen mesh wick with 180 (outer mesh) + 180 (inner mesh).

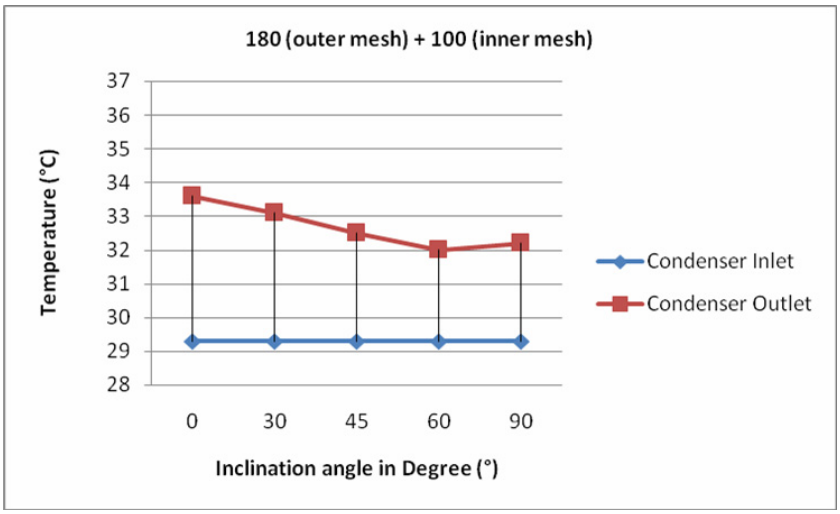

Figure 7. Double layer wrapped screen mesh wick with 180 (outer mesh) + 100 (inner mesh).

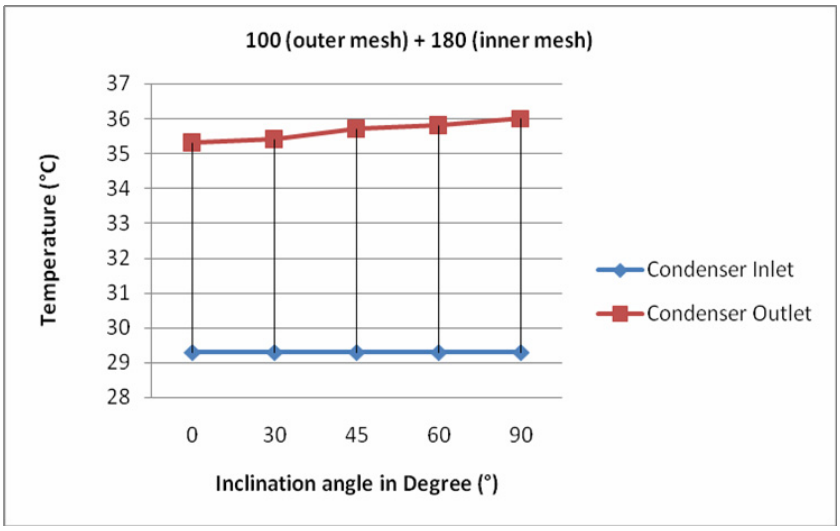

Figure 8. Double layer wrapped screen mesh wick with 100 (outer mesh) + 180 (inner mesh).

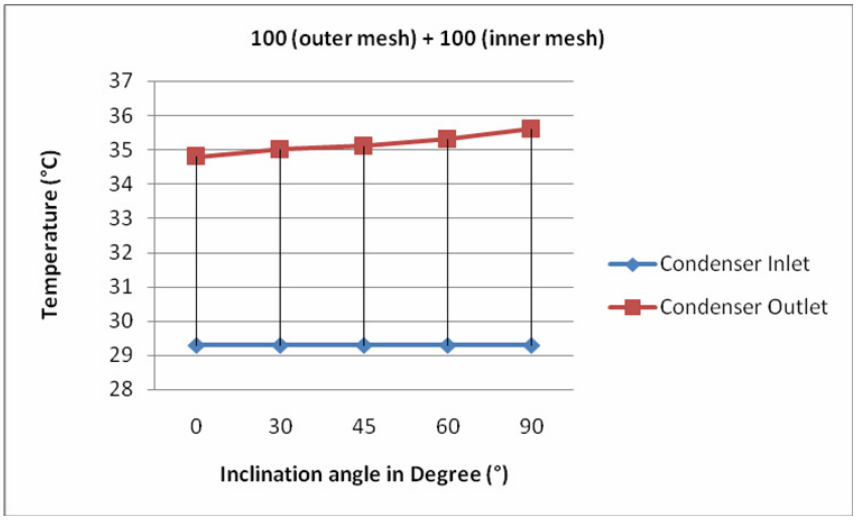

Figure 9. Double layer wrapped screen mesh wick with 100 (outer mesh) + 100 (inner mesh).

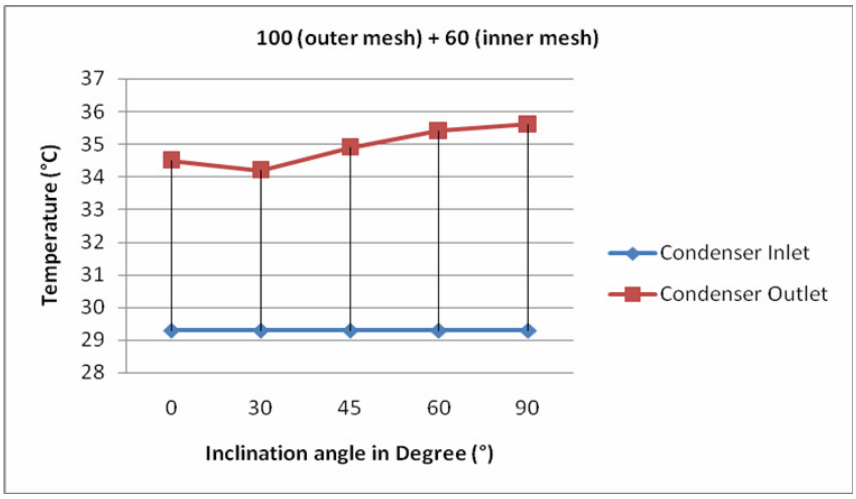

Figure 10. Double layer wrapped screen mesh wick with 100 (outer mesh) + 60 (inner mesh).

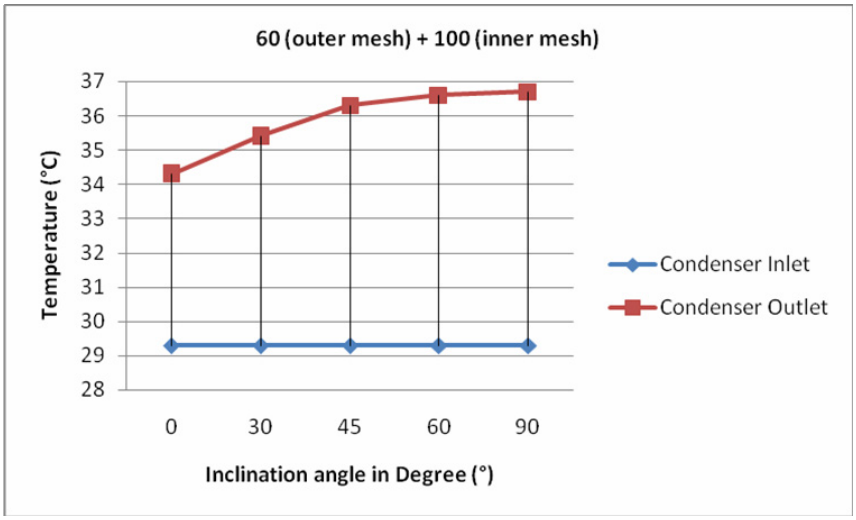

Figure 11. Double layer wrapped screen mesh wick with 60 (outer mesh) + 100 (inner mesh).

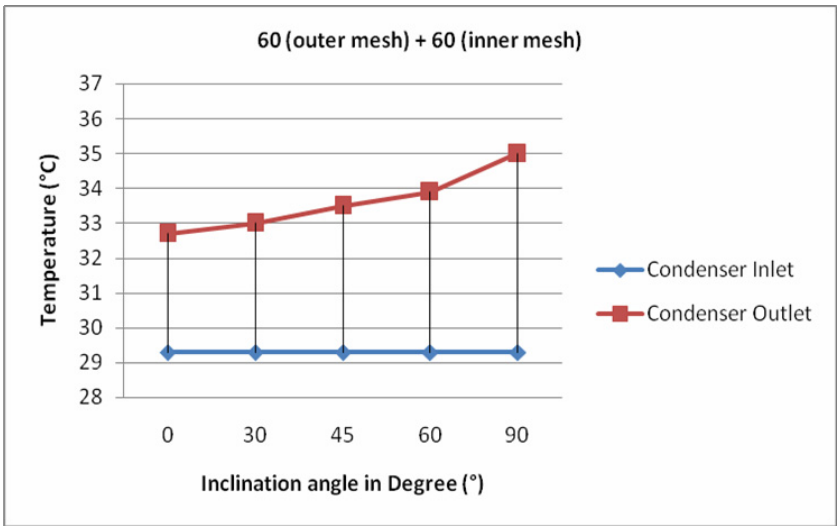

Figure 12. Double layer wrapped screen mesh wick with 60 (outer mesh) + 60 (inner mesh).

Results of dissimilar combination of double wrapped screen mesh of heat pipe shown with temperature versus inclination angle of heat pipe. Among above results the combination of 60 (outer mesh) + 100 (inner mesh) revealed highest temperature difference between condenser inlet and condenser outlet water temperature of cooling jacket. Subsequently 100 (outer mesh) + 180 (inner mesh) and 100 (outer mesh) + 100 (inner mesh) are present higher temperature difference between condenser inlet and condenser outlet. Most of the combinations of double layer wrapped screen mesh shows better result at inclination angle of 90°, i.e., evaporator section is exactly below the condenser section of heat pipe. Charts also show better results if use of coarse mesh at outer side (wall side) and fine mesh at inner side (liquid side), i.e., 180 (outer mesh) + 250 (inner mesh) afford better result than 250 (outer mesh) + 250 (inner mesh) and 250 (outer mesh) + 180 (inner mesh) combination in double layer wrapped screen mesh.

3.1. Heat transfer limits of heat pipe

Study the parameters and phenomenon occurrence of homogeneous nucleation and boiling limitation in the operation of heat pipe. The parameter

nucleation radius of vapor bubble determined for capillary structure, heat pipe enclosure and working fluid. The microscopic cavities with entrapped non condensed gases effect on early occurrence of the boiling phenomenon, so use tested liquid and surface to high static pressure, liquid degassing, on non condensable gas evacuation, small gaps between the envelope and wick or well fabricated heat pipe can avoid the nucleation boiling. The liquid superheat temperature or homogeneous nucleation can be accurately calculated with classical model, i.e., the value of the liquid surface tension, an equilibrium property of the macroscopic interface and Kwak model, i.e., surface energy for vapor bubble formation. The superheat limit depends only on the physical properties of the liquid and vapor temperature [10].

The operation of heat pipe elaborated using different parameters of heat pipe for calculation and equations. The results are plot with stream function, temperature, velocity components, pressure, and shear rate against axial distance at different Reynolds number. The stream function and temperature increase linearly in evaporator section, steady in adiabatic section, decrease linearly in condenser section. The pressure distribution and shear rate decrease linearly in evaporator section, steady in adiabatic section, increase linearly in condenser section [11].

Table 2. Thermodynamic properties of water at working temperature of 30°C

Vapor pressure P_v	Latent heat h_{fg}	Liquid density ρ_l	Vapor density ρ_v	Liquid thermal conductivity k_l	Liquid viscosity μ_l	Vapor viscosity μ_v	Liquid surface tension σ
4500 Pa	2425×10^3 J/kg	995.25 kg/m^3	0.035 kg/m^3	0.6165 W/m·K	0.825×10^{-3} kg/m·s	1×10^{-5} kg/m·s	7.12×10^{-2} N/m

Performance and behavior of heat pipe are demonstrated with numerical analysis of mass and heat transfer. The plan of temperature, concentration, stream function, vorticity function, velocity component versus axial distance at various Reynolds numbers, shows an increase in evaporator section, decrease in condenser section and nearly constant in adiabatic section with increase in axial distance. The plan of pressure, shear rate versus axial

distance at various Reynolds numbers, shows a negative decrease in evaporator section, negative increase in condenser section and nearly constant in adiabatic section with increase in axial distance [12].

Table 3. Capillary limit at different inclination angle

Sr. No.	Wrapped Screen Mesh type (outer + inner)	Capillary Limit in Watt at Different Inclination				
		90°	60°	45°	30°	0°
1	250+250	19.083	18.081	16.747	14.967	10.576
2	250+180	64.676	61.276	56.757	50.725	35.843
3	180+250	64.676	61.276	56.757	50.725	35.843
4	180+180	54.991	51.601	47.079	41.047	26.165
5	180+100	248.701	233.281	212.814	185.276	118.205
6	100+180	248.701	233.281	212.814	185.516	118.205
7	100+100	248.572	229.22	203.588	169.413	85.177
8	100+60	888.948	819	727.291	604.748	302.876
9	60+100	888.948	819	727.291	604.748	302.876
10	60+60	965.902	880.438	765.64	611.657	236.077

Table 4. Different heat transfer limit at 90° inclination with evaporator exactly below condenser and operating temperature 30°C

Sr. No.	Wrapped Screen Mesh (Outer + inner)	Wick Permea-bility	Porosity	Capillary Limit (W)	Sonic Limit (W)	Entrainment Limit (W)	Effective Thermal Conductivity	Boiling Limit (W)	Viscous Limit (W)	Total Thermal Resistance (°C/W)
1	250+250	2.609×10^{-11}	0.5751	19.083	1263.38	505.33	1.4635	41960	49711.443	0.10496
2	250+180	8.842×10^{-11}	0.6939	64.676	1263.38	505.33	1.4635	41960	49711. 44	0.10496
3	180+250	8.842×10^{-11}	0.6939	64.676	1263.38	505.33	1.1282	32492.3	49711.443	0.1331
4	180+180	8.842×10^{-11}	0.6939	54.991	1263.38	505.33	1.1282	32492.3	49711.443	0.1331
5	180+100	2.733×10^{-10}	0.6831	248.701	1213.62	399.65	1.197	23085.69	45896.791	0.186
6	100+180	2.733×10^{-10}	0.6831	248.701	1213.62	399.65	1.154	21672.65	45896.791	0.186
7	100+100	2.733×10^{-10}	0.6831	248.572	1174.09	334.12	1.154	17525.86	42933.056	0.2382
8	100+60	7.332×10^{-10}	0.6756	888.948	1108.59	279.15	1.625	12855.94	38245.985	0.326
9	60+100	7.332×10^{-10}	0.6753	888.948	1108.59	279.15	1.73	19151.12	38245.985	0.326
10	60+60	7.332×10^{-10}	0.6753	965.902	1044.12	234.19	1.1734	10149.71	33953.584	0.404

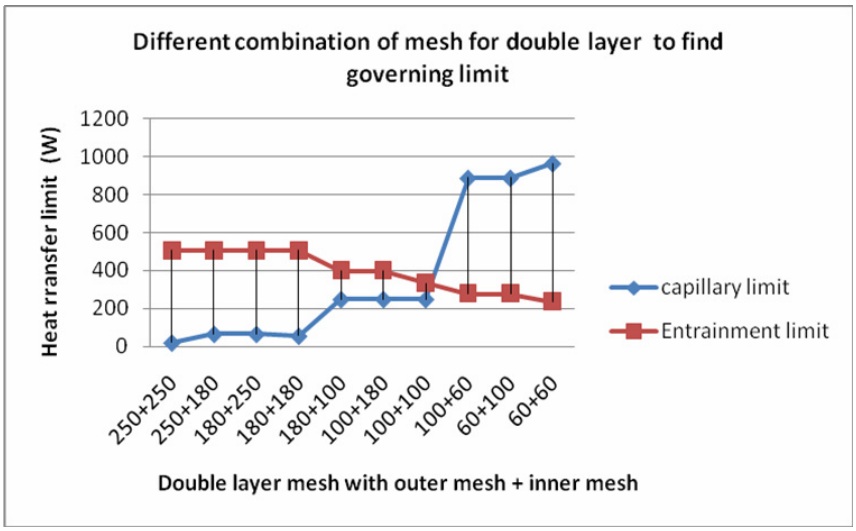

Figure 13. Variation of governing limit with different combination of mesh for double layer.

The heat pipe used water as working fluid for all 10 heat pipes at operating temperature 30°C. The thermodynamic properties of water at operating temperature 30°C can be noted from Table 2. The capillary limit detect high at inclination angle 90° in all combination cases of double layer mesh from Table 3. The governing limit for heat pipe among capillary limit, sonic limit, entrainment limit, viscous limit and boiling limit is the minimum limit within these limits. From Table 4, it easily view except combination of 60 mesh other combination operate with capillary limit as governing limit and for combination of 60 mesh operate with entrainment limit as governing limit.

3.2. Mechanism of porous media in double layer wrapped screen mesh

Using Darcy's law and Knudsen diffusion, the mechanism of porous media of wrapped screen mesh is explained quickly and easily. Darcy's law illustrates the flow through porous medium with equation state that total discharge is proportional to the permeability of the medium and pressure gradient. So here mesh of porous media of wrapped screen mesh having different permeability structures like 60 mesh, 100 mesh, 180 mesh and 250

mesh. The law states higher the permeability higher will be the total discharge through porous medium, means higher discharge of hot fluid from wall side to inner side of heat pipe. Consequently use of higher permeability structure at wall side will provide better heat extraction from hot wall of heat pipe. As a result, charts of temperature versus inclination show better result or higher temperature difference at mesh having higher permeability, i.e., 100 mesh than 180 mesh, 180 mesh than 250 mesh (where combine mesh governing limit is capillary limit other than 60 combine mesh as shown in Table 4, i.e., as capillary limit directly concern with wick structure Table 4). Although high permeability mesh provides better results, the results can increase if structure provides high pressure gradient as Darcy's law states, i.e., along this mesh using higher mesh size to develop higher pressure gradient. For that reason, total discharge increases with using fine porous mesh (higher mesh size) at the inner side of double layer wrapped screen mesh and higher permeability mesh at outer side. Hence, results of temperature versus inclination show better result or higher temperature difference at 100 outer mesh + 180 inner mesh combination than the combine mesh of 100 inner mesh + 100 outer mesh and combine mesh of 180 outer mesh + 100 inner mesh. And same for different combination of 250 mesh, 180 mesh, 100 mesh provide better result of mesh having higher permeability at outer side and fine porous mesh (higher mesh size) at inner side of heat pipe.

In view of that 60 mesh wrapped screen mesh provides larger permeability size than the other mesh of 100 mesh, 180 mesh and 250 mesh (combinations of 60 mesh have governing limit of entrainment limit as shown in Table 4). So 60 mesh provides the larger total discharge as compare to others from wall side to inner side of heat pipe, i.e., transfer more hot fluid to inner side of heat pipe. Hence, results of temperature versus inclination show better result or higher temperature difference at 60 inner mesh + 100 outer mesh combination than the combine mesh of 60 inner mesh + 60 outer mesh and combine mesh 100 outer mesh + 60 inner mesh. As a result among different combinations of outer mesh (high permeability) and inner mesh

(fine porous mesh, i.e., higher mesh size), combine mesh of 60 outer mesh + 100 inner mesh providing best result or highest temperature difference in temperature versus inclination charts. 60 combinations wick structure have higher capillary limit than combinations of 100, 180 and 250. Higher the wick thicknesses have higher capability to hold in heat pipes, also the boiling limit is greater in case of combination of 60 outer and 100 inner meshes than combination of 100 outer and 60 inner meshes.

Knudsen diffusion for porous media of wrapped screen mesh states that gas molecules collide with the porous media frequently than with each other. When the temperature is increased, the velocity in these collisions also increased. In steady state, the ratio of pressure to square root of temperature is same for hot side and cold side. Here the vapor bubbles generated at outer mesh of heat pipe collide more with the mesh of higher mesh size, i.e., smaller pore diameter and increase temperature of the inner mesh which in contact with the liquid in heat pipe. The heat transfer increasing from inner mesh wick to liquid as the temperature of wick increasing and reduction in the vapor bubbles in flow. The drop in percentage of vapor bubbles in flow increase heat transfer as heat transfer is more in liquid than gases. Besides sucking effect formed due to smaller pore diameter at inner side than bigger pore diameter at outer side, subsequently liquid flow increases from outer side to inner side. Consequently the use of higher mesh at inner side provides more heat transfer stability in combination of inner mesh and outer mesh.

3.3. CFD result and discussion

The experimental results of air cooled condenser shown using copper container and wick material with water as working fluid at different heat input and compared with the results of CFD software. The CFD analysis done with the model of heat pipe and using governing equations of vapor flow region, liquid flow region and heat pipe wall region. Graphs show the decrease in the temperature of surface temperature distribution and vapor temperature distribution along the axial direction with respective to time but increase in the temperature in adiabatic section of the vapor temperature distribution [13].

The different working fluids of heat pipe at various flow stream calculation analyzed for enhance thermal performance of heat pipe. The analysis based on internal fluid flow profiles, air temperature profiles, rate of heat transfer and validation based on CFD results. In testing for internal fluid flow profiles, among different working fluids (water, ethanol, R134a), water has the lowest ratio of volume fraction and ethanol has highest velocity. Working fluids show parabolic increase in temperature and among fluids R134a reaches its maximum temperature for various high wall source temperatures. In testing of air temperature profile, at all ranges of source temperature as water displayed the highest reduction in air temperature of all the compared fluids and it increased for all fluid with increase in source temperature. In calculation for rate of heat transfer, water shows the maximum heat exchanger effectiveness and superior heat transfer capability among different working fluid. Using comparison of CFD data and experimental data, validation done on the basis of minimum errors [14].

The two phase flow in flat heat pipe along mathematical modeling analyzing steady state performance with experimental, CFD results, Nusselt number and Sherwood number. Vapor velocity is scheme against centerline; it shows that velocity increases in evaporator section and decreases in condenser section with constant in adiabatic section. Liquid velocity is scheme against wick centre line, which shows that velocity increases in condenser section and decreases in evaporator section with nearly constant in adiabatic section. In boiling of Nusselt number scheme against wall saturation, graph decreases with increase in wall saturation. In condensing Nusselt number scheme against wall saturation, graph increases with increase in wall saturation. In boiling of Sherwood number scheme against wall saturation, graph decreases with increase in wall saturation. In condensing Sherwood number scheme against wall saturation, graph increases with increase in wall saturation [15].

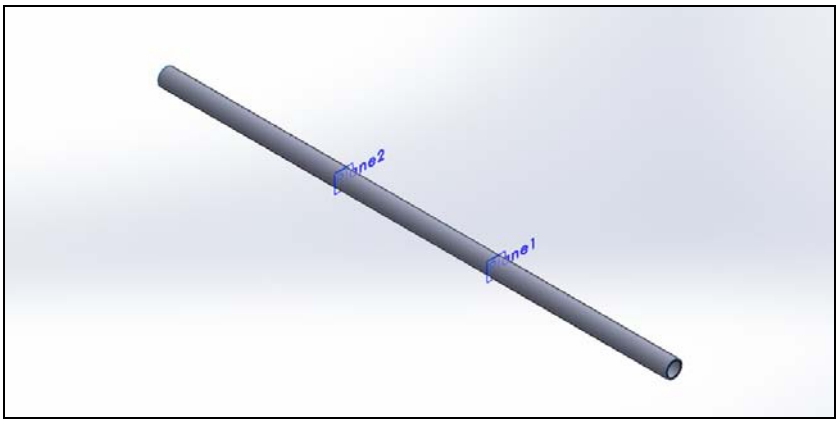

Figure 14. Modeling of heat pipe with planes.

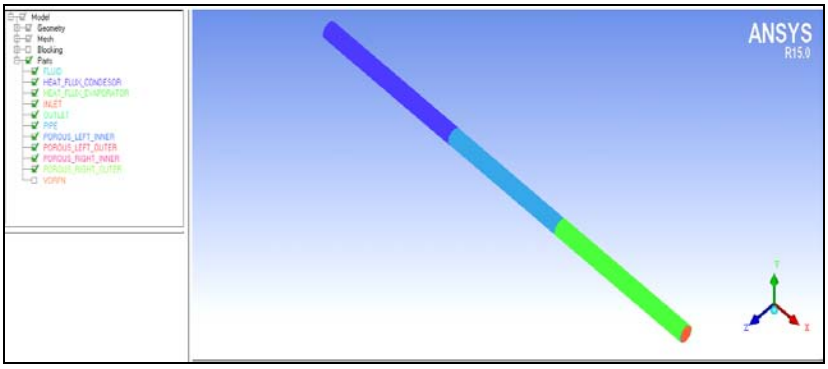

Figure 15. Mesh of different parts with double layer wick mesh of heat pipe.

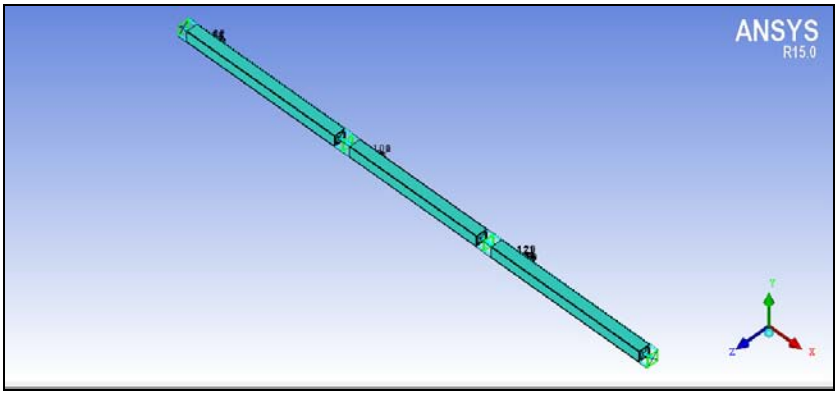

Figure 16. Blocking of the heat pipe parts.

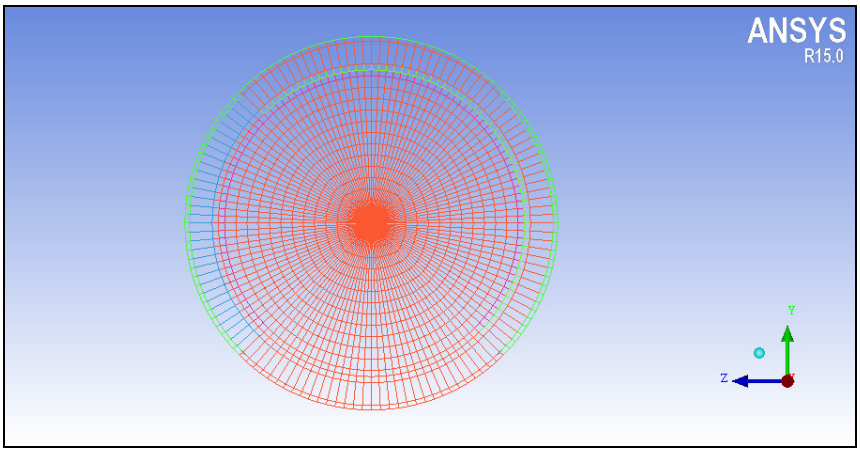

Figure 17. Structured mesh (hexa hedral) of heat pipe.

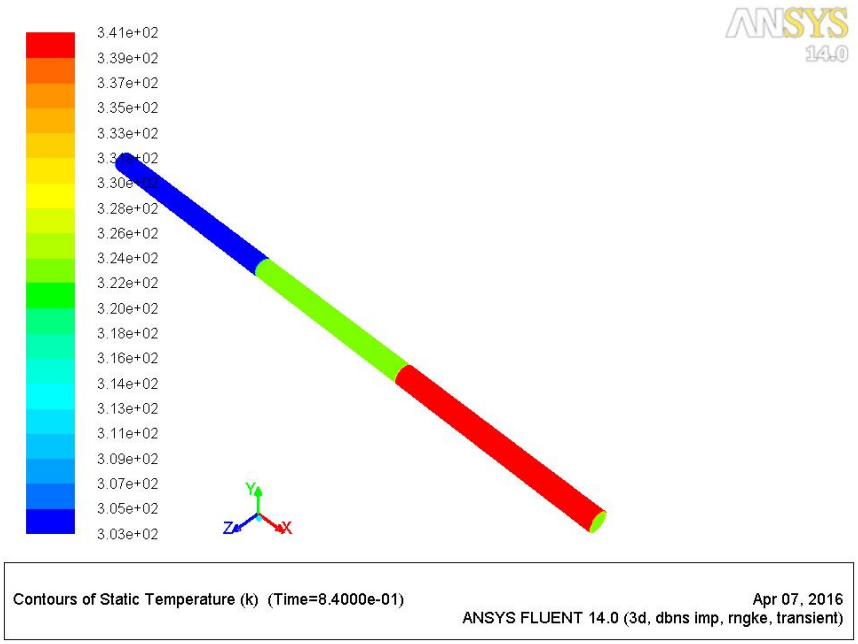

Figure 18. Contours of static temperature for heat pipe.

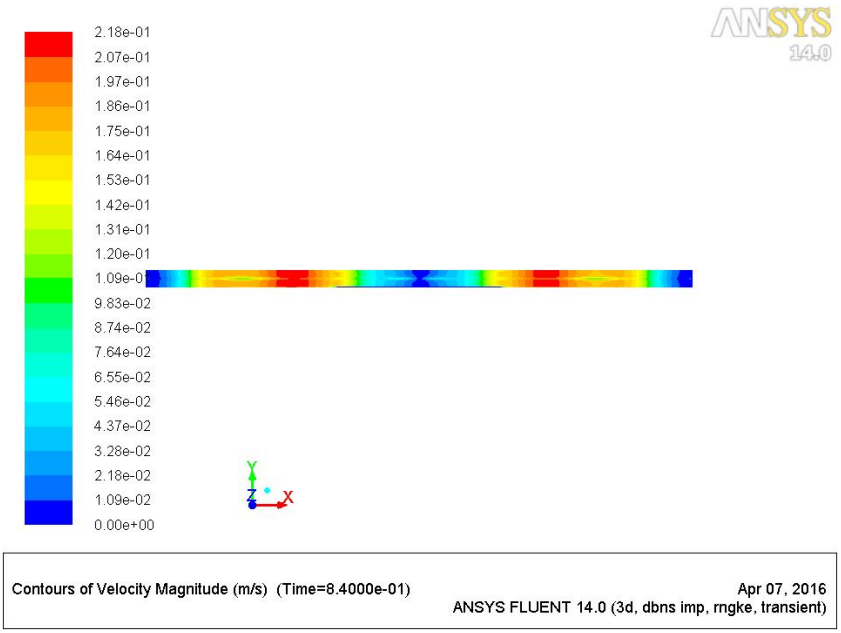

Figure 19. Contours of velocity magnitude inside the heat pipe.

For CFD simulation, here use ANSYS FLUENT 14.0 with heat transfer module and multiphase module. The parts in modeling of heat pipe are the pipe, cooling section on condenser, heating section on evaporator, double layer of porous wick on both sides except adiabatic section, and close inlet, close outlet. In contours of static temperature for heat pipe directly indicate evaporator section (most heated, i.e., highest temperature) and condenser section (most cooled, i.e., lowest temperature). In contours of velocity magnitude inside heat pipe shows highest velocity near porous media in both evaporator and condenser section and due to entrainment limit action lowest velocity magnitude at center of heat pipe, i.e., in adiabatic section.

4. Conclusions

Analyzing all heat pipes with keeping the same dimension with varying wick mesh of double layer wrapped screen mesh. Results and discussion based on the experimental results and analytical study is to find the best combination of double layer wrapped screen mesh. To the above reference conclusions made are:

(1) Fine mesh 250 (outer mesh) + 250 (inner mesh) operate at heat input of 19 watt below required 45 watt, accordingly the design of heat pipe should be changed. The governing limit of heat pipe for excluding 60 mesh combinations operate with capillary limit and for 60 mesh combinations operate with entrainment limit. The capillary limit examines highest value at the inclination angle of 90° of heat pipes.

(2) The combination of 60 (outer mesh) + 100 (inner mesh) provides the best result among all heat pipes as it provides high permeability mesh at outer side and fine mesh at inner side of double layer wrapped screen mesh. Analyzing properly the phenomenon of vapor blanket layer formation, vapor percentage can be reduced in the flow which increases the heat transfer in the flow.

(3) If heat input applied to heat pipe at near its governing limit, the result in reducing evaporator temperature in its control limit or design limit of 60 to 70 degree celsius as in 180 (outer mesh) + 180 (inner mesh). As heat input applied is 45W and governing limit of 180 (outer mesh) + 180 (inner mesh) is 54.991W.

Acknowledgement

The authors thank the anonymous referees for their valuable suggestions and constructive criticisms towards the improvement of the manuscript.

References

[1] Jinliang Wang and Ivan Catton, Biporous heat pipes for high power electronic device cooling, Seventeenth IEEE SEMI-THERM Symposium, 2001.

[2] Jeehoon Choi, Yuan Yuan, Wataru Sano and Diana-Andra Borca-Tasciuc, Low temperature sintering of copper biporous wicks with improved maximum capillary pressure, Materials Letters 132 (2014), 349-352.

[3] Brian Holley and Amir Faghri, Permeability and effective pore radius measurements for heat pipe and fuel cell applications, Applied Thermal Engineering 26 (2006), 448-462.

[4] K. C. Leong and C. Y. Liu, Characterization of sintered copper wicks used in heat pipes, Journal of Porous Materials 4 (1997), 303-308.

[5] C. Ferrandi, F. Iorizzo, M. Mameli, S. Zinna and M. Marengo, Lumped parameter model of sintered heat pipe: Transient numerical analysis and validation, Applied Thermal Engineering 50 (2013), 1280-1290.

[6] Wei Liu, Zhi Chun Liu, Kun Yang and Zheng Kai Tu, Phase change driving mechanism and modeling for heat pipe with porous wick, Chinese Science Bulletin 54(21) (2009), 4000.

[7] K. Vafai and W. Wang, Analysis of flow and heat transfer characteristics of an asymmetrical flat plate heat pipe, Int. J. Heat Mass Transfer 35(9) (1992), 2087-2099.

[8] Douglas R. Adkins and Ronaid C. Dykhuizen, Procedures for measuring the properties of heat-pipe wick materials, AIIM 301/587-8202.

[9] Qingjun Cai and Ya-Chi Chen, Investigations of biporous wick structure dryout, J. Heat Transfer 134(2) (2011), 8.

[10] D. Mishkinis and J. M. Ochterbeck, Homogeneous nucleation and the heat-pipe boiling limitation, Journal of Engineering Physics and Thermophysics 76(4) (2003), 813-818.

[11] Selah M. Salih, Qahtan A. Abed and Dhafeer M. Al-Shamkhi, Numerical analysis of vapor flow in a horizontal cylinderical heat pipe, Al-Qadisiya Journal for Engineering Sciences 4(3) (2011), 233-247.

[12] R. Rajashree and K. Sankara Rao, A numerical study of the performance of heat pipe, Indian J. Pure Appl. Math., 21(1) (1990), 95-108.

[13] Arul Selvan Annamalai and Velraj Ramalingam, Experimental investigation and computational fluid dynamics analysis of an air cooled condenser heat pipe, Thermal Science 15(3) (2011), 759-772.

[14] Hassam Nasarullah Chaudhry and Ben Richard Hughes, Analysis of the thermal cooling capacity of heat pipes under a low Reynolds number flow, Applied Thermal Engineering 71(1) (2014), 559-572.

[15] Rakesh Hari and C. Muraleedharan, Numerical analysis of two phase flow in flat heat pipe, International Journal of Innovative Research in Science, Engineering and Technology 2(1) (2013), 702-709.